Article

Crystal plasticity with micromorphic regularization in assessing scale dependent deformation of polycrystalline doped copper alloys

Matti Lindroos[1], Tom Andersson[1], Jarkko Metsäjoki[1], Anssi Laukkanen[1]

[1] Integrated Computational Materials Engineering, VTT Technical Research Centre of Finland Ltd.
* Correspondence: Tom Andersson; Tel.: +358 40 7702369

Abstract: Doped copper overpacks are planned to be utilized in the spent nuclear fuel repositories in Finland and in Sweden. The assessment of long-term integrity of the material is a matter of importance. Grain structure variations, segregation and any possible manufacturing defects in microstructure are relevant in terms of susceptibility to creep and damage from the loading evolution imposed by its operating environment. This work focuses on studying the microstructure level length-scale dependent deformation behavior of the material, of particular significance with respect to accumulation of plasticity over the extensive operational period of the overpacks. Reduced micromorphic crystal plasticity model, which is similar to strain gradient models, is used in this investigation. Firstly, the model's size dependent plasticity effects are evaluated. Secondly, different microstructural aggregates presenting overpack sections are analyzed. Grain size dependent hardening responses, i.e., Hall-Petch like behavior, can be achieved with the enhanced hardening associated with the micromorphic model at polycrystalline level. It was found that the nominally large grain size in the base material of the overpack shows lower strain hardening potential than the fine grained region of the welded microstructure with stronger strain gradient related hardening effects. Size dependent regularization of strain localization networks is indicated as a desired characteristics of the model. The findings can be utilized to provide an improved basis for modeling the viscoplastic deformation behavior of the studied copper alloy and assess the microstructural origins of any integrity concerns explicitly by way of full field modeling.

Keywords: micromechanics; crystal plasticity; micromorphic; Hall-Petch; copper alloys;

1. Introduction

Regarding the spent nuclear fuel repository in Finland, the copper overpack of the canister will be an important barrier against radioactive discharge from the repository. Final disposal overpacks are placed to a cave in bedrock at a depth of approximately 400 meters [1]. The overpack is surrounded by bentonite blocks that swell due to the ground water. As the hydrostatic and bentonite swelling pressure will develop overpack will be pressed against the insert, affecting the stress state in the overpack. High purity oxygen-free phosphorus-doped (OFP) copper is the intended material for the overpack to reduce the amount of Cu_2O inclusions. The phosphorous is added to further reduce the inclusion since as the hydrogen diffuses through the copper its can react with the Cu_2O inclusions, forming H_2O steam bubbles at the grain boundaries.The overpack will be internally heated up to 100°C by residual nuclear fuel activity and thus time-dependent deformation and damage mechanisms (creep, stress relaxation and cyclic loads) are active during its operational lifetime.

The creep behavior of OFP copper has been extensively studied over the years due to the immediate concerns to ensure integrity in the final disposal applications. These works have focused on both experimental campaigns and development of modeling and integrity analysis methods, as in, for example, [2,3]. Typically, the respective works have not explicitly treated material plasticity and creep at the scale of the microstructure, but rather presented "top-down" like approaches to assess the behavior of bulk material, discontinuities such as welds and focused on extrapolation of the experimental results towards long-term operational periods. Simultaneously, strategies have been developed to better integrate more complex creep models to integrity analyses ([4,5]) to account for different stages of creep (such as extensive primary creep exhibited by several relevant copper alloys, [3]) and effects of joints and welds via concepts such as the weld strength factor (WSF). However, none of these nor other earlier works have performed direct modeling of plasticity at the scale of the microstructure, rather identified the possible need to further the respective capabilities to improve upon the respective predictive nature of the used material models and approach rather in a somewhat more physics-based manner.

Micromechanical modelling, on the other hand, provides the basis for microstructure informed modelling of creep incorporating plastic deformation (slip) and the damage (cumulative microstructure scale creep-fatigue damage). In current work, microstructural and crystal plasticity (CP) modelling of OFP copper will be utilized and its performance in reproducing experimentally determined stress and strain response is presented. CP models can be employed to investigate the microscale deformation, hardening and eventually susceptibility to damage. To address the grain size dependencies of the material, often a Hall-Petch type relation is introduced in the models, which defines yield offset to match grain size dependent yielding behavior and link grain size with the evolution of dislocation density [6]. Alternatively, length-scale dependent plasticity models can be utilized [7, 8]. Constitutive relations are modified to represent storage of geometrically necessary dislocations (GND) within crystal plasticity framework [9,10]. Use of full dislocation density tensor is possible to capture size effects at the level of microstructure to analyze grain-grain interactions or the role of defects [11,12]. Similar size dependent effects are obtainable with Micromorphic theory originally proposed in [13] and [14] and further developed in [15]. Besides size dependent hardening behavior, the regularization of strain localization is key target of these models and the associated softening in the shear bands. Current work does not directly account for damage accumulation at the scale of the material microstructure, although this is a direct extension of the proposed approach also in the case of OFP copper alloys [16], and is foreseen to improve upon the capabilities in assessing the interactions between plasticity and defect structures especially critical in welds of the overpack structure.

This work uses a reduced micromorphic model with a scalar variable linked to strain gradient effects, which is introduced in Section 2.1. Such models have been developed in the past [17–19] to reduce the computational cost of the length-scale dependent models. As a novel feature, we investigate the deformation and strain hardening behavior of copper overpack material at the polycrystalline level. The microstructure of the material varies depending on the section of the cylindrical shaped overpack, whether the base material of the cylinder/lid parts are analyzed or the friction stir welded zone is a matter of interest. Results are divided into two main topics. Section 3.2 focuses on the scaling capability of the micromorphic model with electron back-scatter diffraction (EBSD) based realistic microstructural aggregates. In the final result Section 3.3, we perform simulated tensile tests to the different overpack microstructures to analyze strain hardening, stress and strain localization behavior. The role of enhanced hardening model is discussed and observations on the relevant plastic deformation behavior of the investigated microstructures are provided.

2. Materials and Methods

2.1. Crystal plasticity modeling

A finite strain formalism is used with multiplicatively decomposed deformation gradient to elastic and plastic parts:

$$\underset{\sim}{F} = \underset{\sim}{F}^E \cdot \underset{\sim}{F}^P \tag{1}$$

Dislocation slip rate is given by a viscoplastic flow rule. Dislocation driven plasticity occurs by a sum of potentially active twelve $\{111\} < 110 >$ slip systems, given by:

$$\dot{\gamma}^s = \langle \frac{|\tau^s| - (R^s - S_\chi)}{K} \rangle^N sign(\tau^s) \tag{2}$$

where K and N describe viscosity and strain rate dependency, respectively. τ^s is the resolved shear stress on a slip system s. A conventional isotropic hardening contribution is defined by R^s. The generalized stress S_χ provides another source of isotropic hardening for the slip system. The theoretical and thermodynamic derivation of the strain gradient extension S_χ is provided in ref. [18]. Alternative formulation of similar kind of strain gradient extension using so-called augmented Lagrangian method can be found in [20]. The key aspect of the present reduced Micromorphic strain gradient model is essentially to provide scale dependent regularization on plastic slip. This characteristically provides scale dependent hardening behavior, which we employ in this work to further the realism in modeling polycrystalline OFP copper microstructures. The major difference in this work is that we investigate the model behavior for polycrystalline copper, while the referred to previous studies have focused on the regularization of local slip bands and to analyze the model characteristics and effects of micromorphic parameters.

The regularization of slip is established with an additional strain-like scalar variable *microslip* γ_χ introduced as a degree of freedom (DOF) [18] in addition to the standard displacement DOFs. A cumulative plastic slip term γ_{cum} is defined as:

$$\gamma_{cum} = \int_0^t \sum_s^{N^s} |\dot{\gamma}^s| dt \tag{3}$$

γ_{cum} and *microslip* γ_χ are related by a regularization equation [18]:

$$\gamma_\chi - \frac{A}{H_\chi} \Delta_\chi \gamma_\chi = \gamma_{cum} \tag{4}$$

where Δ_χ is Lagrangian Laplace type operator. Micromorphic parameters A and H_χ control the gradient effect. Their more detailed meaning and influence on slip localization are discussed in [19]. It can then be derived that the generalized stress affecting slip activity becomes:

$$S_\chi = -H_\chi(\gamma_{cum} - \gamma_\chi) \tag{5}$$

If the penalization parameter H_χ is chosen high enough, the Micromorphic model extension in fact resembles classical strain gradient plasticity [21]. In such a case, γ_χ becomes almost equal to γ_{cum}.

The classical isotropic hardening related to Hall-Petch behavior and dislocation interactions is given by:

$$R^s = \tau_{HP} + \mu \sqrt{\sum_{s=1}^{N^s} a^{sr} \rho^r} \tag{6}$$

In order to produce increase in the yield stress, a common Hall-Petch yield offset is introduced. The strain gradient model evokes scale dependent material behavior once plastic strain begins to accumulate. Therefore, the initial yield condition depends on the assigned initial dislocation density and the offsetting given by the Hall-Petch term. In section 3.2, we study the stress-strain response of the material with and without the Hall-Petch offset condition to show the hardening response associated with the length-scale:

$$\tau_{HP} = \frac{\mu}{\mu_{ref}} \frac{K_{HP}}{d} \tag{7}$$

where μ_{ref} is the reference value for shear modulus at room temperature and μ is the current shear modulus value at a specific temperature. Hall-Petch coefficient is K_{HP} and average grain size is d. We assume that solid solution strengthening is included in the Hall-Petch term and we do not introduce it separately.

The evolution of dislocation density is given by:

$$\dot{\rho}^s = |\dot{\gamma}^s| \left(\frac{\sqrt{\sum_{s=1}^{N^s} a^{sr} \rho^r}}{K_{obs}} - G_c \rho^s \right) \tag{8}$$

where parameter K_{obs} describes the strength of obstacles immobilizing dislocations and defines strain hardening curvature. G_c is annihilation distance.

3. Results and discussion

3.1. Material model parameters

The single crystal model parameters were fitted with available experimental data curves from ref. [22] at 75°C, first using a simplified 3D microstructural aggregate and then verified with realistic grain structures in Section 3.3. Figure 1 shows simulated and experimental stress-strain curves after parameter identification. Table 1 lists the simulation parameters for the model.

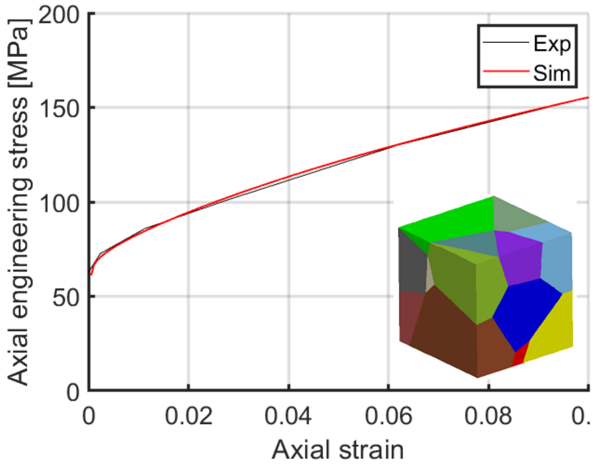

Figure 1. Stress-strain curves of experiments and simulation.

3.2. Model scaling effect

To analyze grain size scaling effects of the model, tensile tests were simulated up to 2% of strain using a subset of an EBSD map as a computational domain. The RVE was scaled to yield different grain sizes for the analysis. Grain size of 150 μm is considered a reference. The range of grain sizes is selected based on those observed in base OFP copper alloys as well as weldments, see for example [3].

Figure 2a,c show stress-strain curves for the chosen grain sizes. In Figure 2a, the initial dislocation density was set equal for each case. The Hall-Petch offset was taken to have a constant value based on 150 μm grain size, which means that no additional offset is included even when the grain size decreases to analyze the effect of the present gradient plasticity extension. Both Figure 2a,b show that the length-scale effects become important already in the microplasticity regime after yielding with a notable influence on the strain hardening rate. Figure 2b shows that the size dependent effects tend to saturate at very small and large grain sizes producing tanh-type of curvature observed in the figure. This behavior is a typical characteristic of the micromorphic crystal plasticity models [23] which have a finite hardening response.

Table 1: Crystal plasticity model parameters

Elasticity		
Elastic constants $[GPa]$	$C_{11} = 168.4$	
	$C_{12} = 121.4$	
	$C_{44} = 75.4$	
Shear modulus $[GPa]$	μ = 42.5	
Plasticity		
Slip parameters		
Viscous parameter	$K\ [MPa.s^{1/n}]$	3.0
Strain rate parameter	N	10.0
Interaction slip-slip	$h_1 - h_6\ \ (H_{rs})$	0.124;0.124;0.625;0.137;0.122;0.07
Hall-Petch coefficient	K_{HP} [MPa $\sqrt{m}$]	0.12
Effective grain size	$d\ [um]$	150.0 or variable
Initial dislocation density	$\rho_0^s\ [m^2]$	$7.63 \cdot 10^{11}$
Dislocation obstacles	K_{obs}	130.0
Dislocation annihilation	$G_c\ [nm]$	10 x b^s
Length of Burgers vector	$b^s\ [m]$	$0.256 \cdot 10^{-9}$
Gradient penalty	$H_\chi\ [MPa]$	10000.0
Gradient parameter	$A\ [MPa.mm^2]$	0.1

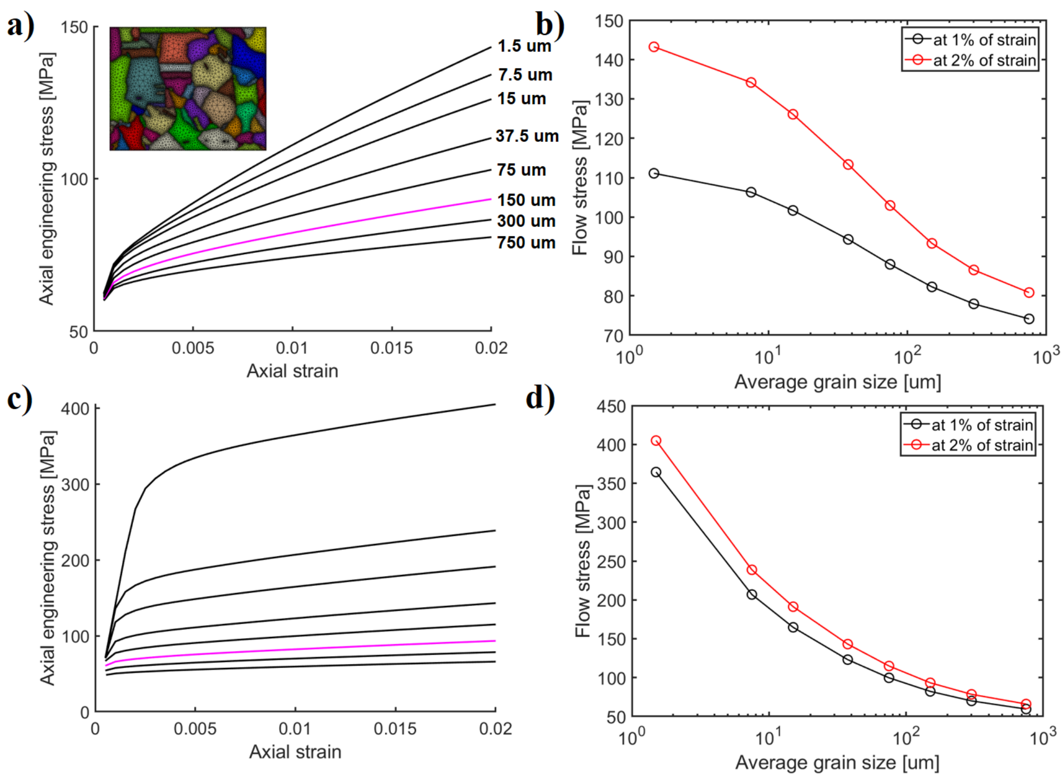

Figure 2. a) Stress-strain curves for different grain sizes without Hall-Petch offset, b) flow stress values at constant strains for different grain sizes, c) stress-strain curves for different grain sizes with Hall-Petch offset, and d) flow stress values at constant strains for different grain sizes using Hall-Petch offset. Computational RVE shown in a) is used for all cases, which is scaled to achieve the specific grain sizes.

3.3. Simulation of copper canister microstructure deformation

The copper overpack material has different microstructural zones depending on the materials processing during manufacturing. Grain size varies depending on the section in the canister and whether the material is being welded at some locations. Tensile simulations were performed on three chosen microstructures. The microstructure A is located within the cylindrical section of the overpack, while B is extracted from the lid section of the overpack. In general, the microstructures are quite similar between A and B containing a mixture of small and large grains. Additionally, a friction stir welded zone was included as a separate simulation since it contains a finer grain size distribution with gradient like refinement in size in the chosen computational domain. It is noteworthy that the welded microstructure can contain this type of refined grain size or alternatively enlarged grain size in some sections of the material, the mismatch of which with respect to resulting viscoplastic strain rates being one additional source for concern and where more detailed modeling tools are required. Additionally, we focus on the small grain size case due to assumption that it has a higher probability to generate high stress concentrations due to the scale dependency. This aspect is also important when analysing the model response with respect to finer grain sizes. The used computational microstructures are shown in Figure 5.

For the A and B cases, we assumed the same average initial grain size of 150 μm and for the friction stir welded zone 102 μm was used. This choice affects the initial Hall-Petch yield offset in the stress-strain curves. Figure 1 shows the stress-strain response of the microstructure cases. It can be seen that the Hall-Petch offset associated differences appear relatively small because the average initial grain size does not have such high variation. The simulated stress-strain curves of microstructure B describe well the experimentally obtained strain hardening behavior.

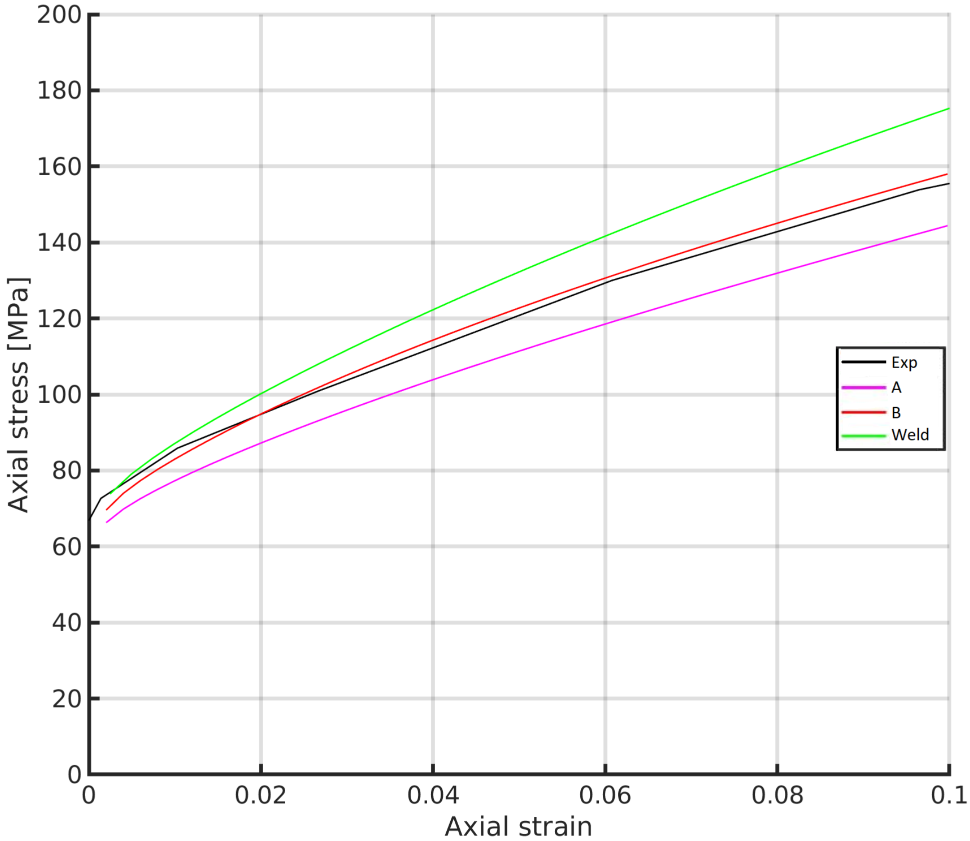

Figure 3. Simulated stress-strain curves for materials A, B and C and experimentally measured curve

Figure 4 shows von Mises stress and cumulative plastic slip at 10% of strain. Inhomogeneous von Mises stress distributions are observed with highest magnitudes at the grain boundaries. Their magnitude tends to decrease towards the cores of the large grains. Smaller grains generate higher stress fields populating almost whole individual grains. For this reason, the welded microstructure shows stronger strain hardening due to the finer overall grain size within the microstructural aggregate. In spite that the microstructures of A and B are quite similar, the hardening responses are slightly different. The microstructure B tends to develop strain localization networks that increase the local dislocation density. The developed strain gradients promote the increase in the generalized stress term affecting the hardening response. This becomes apparent later in Figure 6.

The welded microstructure develops more distinctive inter-grain continuous cumulative plastic slip zones than the A and B microstructures. This result is inline with the observations made by Cordero et al. [23] with a model using full *curl* of the plastic deformation tensor, i.e., so called *microcurl* model. When the grain size decreases, the slip accumulated slip tends to progressively build finite sized strain localization bands until it becomes energetically too expensive at very small grain sizes. At the same time, the scale dependent hardening effectively increases the flow stress which we observe as stronger strain hardening.

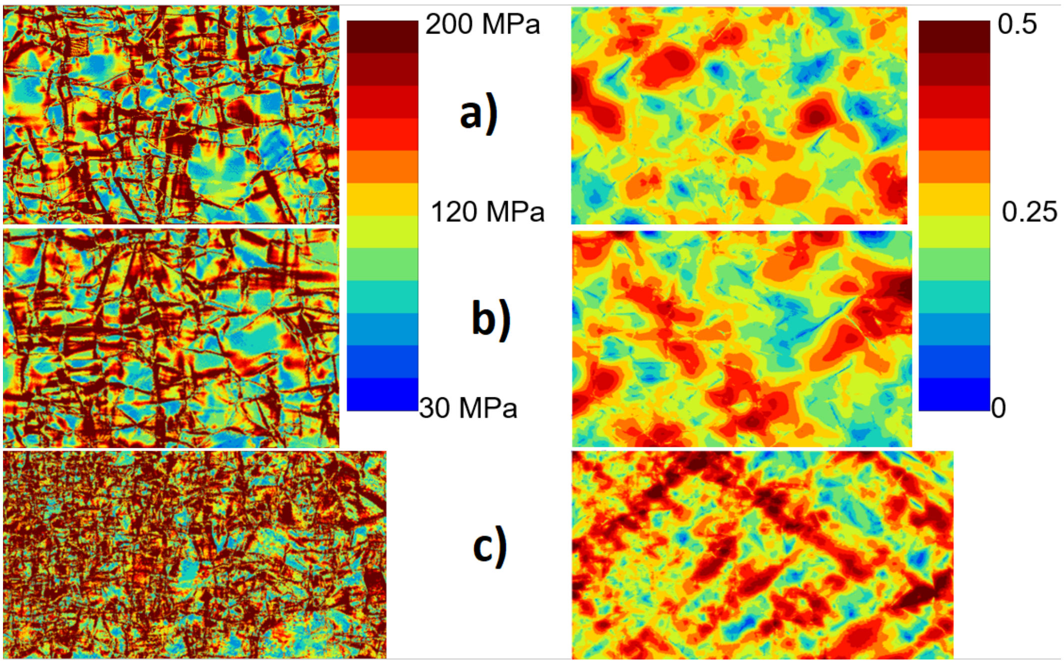

Figure 4. von Mises stress and cumulative plastic slip contours for materials A, B and C

Total dislocation density is plotted at integration point level in Figure 5 at the end of the simulation. It is clear by definition of the dislocation density based slip model that the dislocation density is larger in the zones with high cumulated slip seen in Figure 4. However, Figure 5 shows the dislocation build-up near the grain boundaries. The grains describing hard orientations, i.e., high resistance to slip, with respect to the tensile direction, show lower dislocation densities at the core region of the grains, while at the grain boundaries dislocations accumulate due to neighboring stress concentration effects from interactions with adjacent grains.

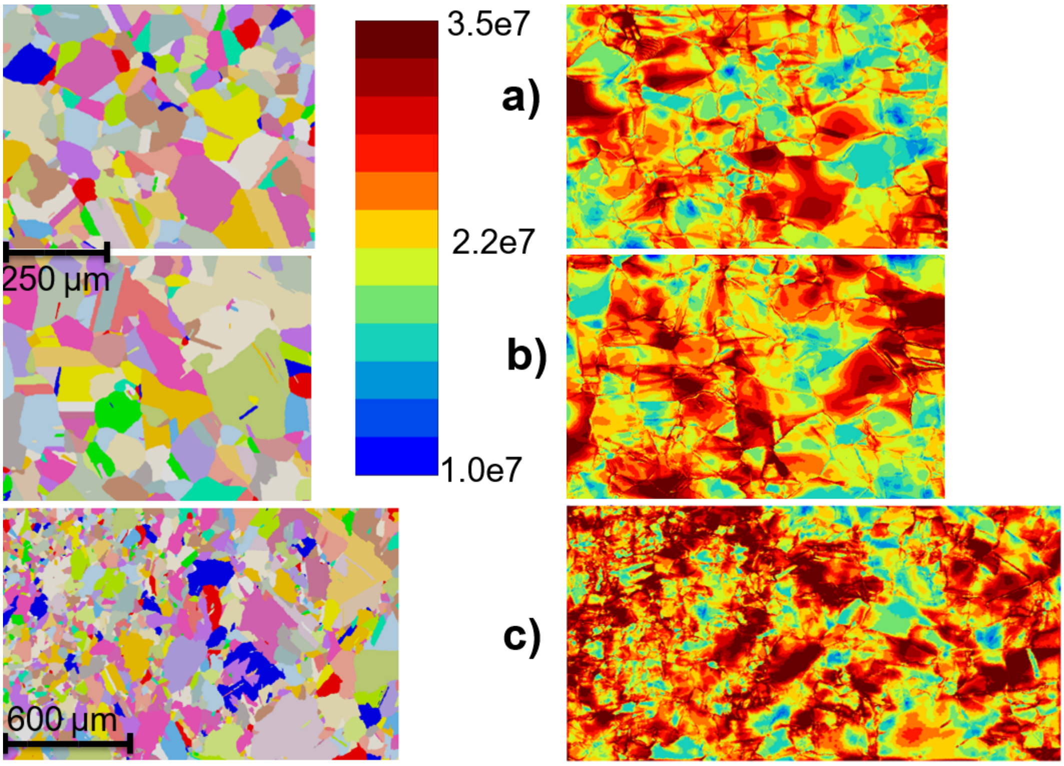

Figure 5. Grain morphology maps and total dislocation density $[1/mm^2]$ contours for materials A (a), B (b), and welded (c).

The average statistically stored dislocation (SSD) densities at the end of simulation were $2.385 \cdot 10^{13}\ 1/m^2$, $2.486 \cdot 10^{13}\ 1/m^2$, $2.620 \cdot 10^{13}\ 1/m^2$, for A, B, and the welded zone, respectively. The values are in the same range and they do not solely explain the difference in the stress-strain curves. The model does not explicitly include geometrically necessary dislocation densities. However, instead the scalar strain gradient related term, as generalized stress S_χ, can be interpreted to play a role in mimicking length-scale hardening dependent effects usually attributed to GNDs.

Figure 6 illustrates the distribution of the generalized stress term S_χ. Recall that S_χ is introduced in Equation 2 that affects slip resistance. It is possible that $R^s - S_\chi < 0$, and therefore we adopt the restriction that $R^s - S_\chi \geq 0$ following [18]. It can be observed that the hardening effect of S_χ is stronger for the microstructure B than A. It should be noted that blue colour (negative sign) produces extra-hardening in Figure 6 with respect to the equation 2. Most significant effect is found near the grain boundaries for larger grains as expected, while smaller grains in 6c show pronounced hardening effect also towards the grain interiors at the fine grained sections of the microstructure. This length-scale dependent model characteristic elevates von Mises stresses as seen in Figure 4.

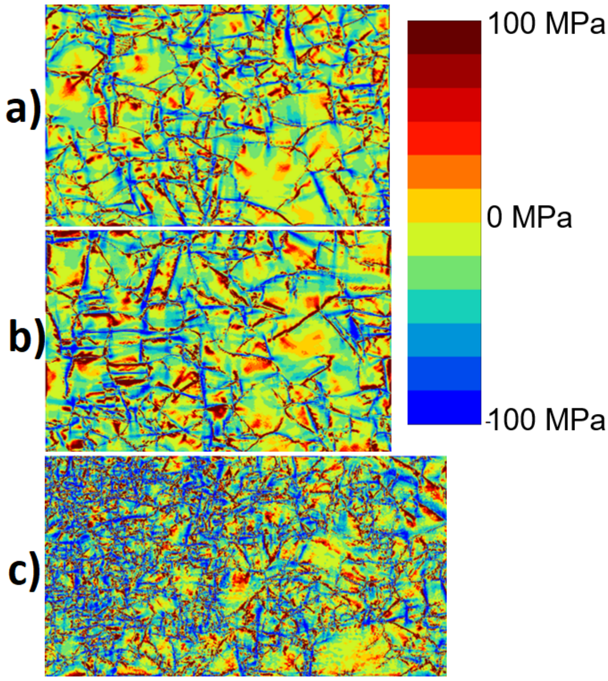

Figure 6. Generalized stress S_χ at 10% of strain for microstructures a) A, b) B, c) welded.

As future scope of work, the model could be used to regularize creep related strain accumulation at the level of microstructure. The assessment of length-scale dependent damage [24] is also a topic requiring attention to have improved estimation of long-term deformation behavior of the copper material and overpack in the final disposal repositories.

4. Conclusions

Reduced micromorphic crystal plasticity model was used to investigate the microstructure scale deformation and hardening response of copper overpack for nuclear fuel repository overpack structures. First, the model feasibility in describing length-scale dependent hardening was analyzed. Then typical microstructural sections from the copper overpack having different microstructures in terms of grain structure/size were analyzed. The following conclusions are made:

- Various length-scale related hardening responses can be achieved with the reduced micromorphic model which is akin to strain gradient models. Significant differences occur with respect to the resulting grain size dependencies. A typical tanh-shaped grain size dependency is obtained with saturation of the hardening at the extreme ends of grain sizes. Intrinsic length-scale then can be adjusted according to the Hall-Petch tanh-curvature when the necessary experimental or multiscale modeling data is available. If the Hall-Petch yield offset is used, the dislocation slip based hardening coming from the length-scale model is masked and the grain size dependent curve resembles a typical square root dependency.
- The modeling approach is usable to investigate grain size dependent plasticity in copper alloys of the overpack having heterogeneous grain distribution in the microstructures. Strain localization is controlled with the model by a regularization placed over plastic slip. The model can produce length-scale dependent plasticity in the range of the typical grain sizes for the material. Greatest hardening accumulates near grain boundaries where dislocation pile-ups are generally expected, and small grains produce further pronounced intra-grain hardening associated with the local spreading of gradient enhanced hardening. The model is computationally robust, however, the limiting feature is that the hardening is introduced mainly as a source of enhanced isotropic hardening in the present context. It is possible to derive a variant to describe more closely kinematic hardening effects [15,18,23].

- Three polycrystalline microstructural aggregates were simulated which represent different sections of the copper overpack, i) cylindrical part of the canister (A), ii) lid of the canister (B), and iii) welded zone. The hardening response of cylindrical and lid regions is quite similar, but the lid contained more small grains that increase strain hardening potential. Welded microstructure has the greatest tendency to develop higher local stresses and distinctive strain localization networks throughout the microstructure.

Author Contributions: Conceptualization, M.L., T.A.; methodology, M.L, T.A., A.L.; simulations, T.A, M.L.; writing and editing, M.L.,T.A.,A.L.; Microstructural characterization, J.M.

Funding: This study was funded by a grant from the Finnish Research Programme on Nuclear Waste Management (KYT 2018 Programme).

Acknowledgments: Prof. Samuel Forest from MINES ParisTech is acknowledged for discussions related to the modeling framework.

Conflicts of Interest: The authors declare no conflict of interest.

References

1. Safety case for the disposal of spent nuclear fuel at Olkiluoto - description of the disposal system. *Posiva 2012-05* **2012**.
2. Uniaxial and Multiaxial Creep Testing of Copper.
3. Material integrity of welded copper overpack–Final report 2011. *VTT 2011, VTT-R-01384-12* **2011**.
4. Holmström, S.; Rantala, J.; Laukkanen, A.; Kolari, K.; Keinänen, H.; Lehtinen, O. Modeling and Verification of Creep Strain and Exhaustion in a Welded Steam Mixer. *Journal of Pressure Vessel Technology* **2009**, *131*.
5. Auerkari, P.; Salonen, J.; Holmström, S.; Laukkanen, A.; Rantala, J.; Nikkarila, R. Creep damage and long term life modelling of an X20 steam line component. *Engineering Failure Analysis* **2013**, *35*, 508–515. Special issue on ICEFA V- Part 1, doi: https://doi.org/10.1016/j.engfailanal.2013.05.008.
6. Monnet, G.; Mai, C. Multiscale modeling of crystal plasticity in steels: Prediction of irradiation hardening. *Journal of Nuclear Materials* **2019**, *514*, 128–138.
7. Fleck, N.; Hutchinson, J. Strain gradient plasticity. *Advances in Applied Mechanics* **1997**, *33*, 296–361.
8. Kocks, U.; Mecking, H. Physics and phenomenology of strain hardening: the FCC case. *Progress in Materials Science* **2003**, *48*, 171 – 273.
9. Ashby, M.F. The deformation of plastically non-homogeneous materials. *The Philosophical Magazine: A Journal of Theoretical Experimental and Applied Physics* **1970**, *21*, 399–424.
10. Acharya, A.; Bassani, J. Lattice incompatibility and a gradient theory of crystal plasticity. *Acta Mater* **2000**, *47*, 11597 – 1611.
11. Gurtin, M.E. A gradient theory of single-crystal viscoplasticity that accounts for geometrically necessary dislocations. *Journal of the Mechanics and Physics of Solids* **2002**, *50*, 5–32.
12. Rys, M.; Forest, S.; Petryk, H. A micromorphic crystal plasticity model with the gradient-enhanced incremental hardening law. *International Journal of Plasticity* **2020**, *128*, 102655.
13. Eringen, A.; Suhubi, E. Nonlinear theory of simple micro-elastic solids—I. *International Journal of Engineering Science* **1964**, *2*, 189–203.
14. MINDLIN, R.D. Micro-structure in linear elasticity. *Archive for Rational Mechanics and Analysis* **1964**, p. 51–78.
15. Forest, S., M.J.M.D. A micromorphic crystal plasticity model with the gradient-enhanced incremental hardening law. *In: Voyiadjis G. (eds) Handbook of Nonlocal Continuum Mechanics for Materials and Structures* **2019**, pp. 643–686.
16. Lindroos, M.; Laukkanen, A.; Andersson, T.; Vaara, J.; Mäntylä, A.; Frondelius, T. Micromechanical modeling of short crack nucleation and growth in high cycle fatigue of martensitic microstructures. *Computational Materials Science* **2019**, *170*, 109185. doi: https://doi.org/10.1016/j.commatsci.2019.109185.
17. Wulfinghoff, S.; Böhlke, T. Equivalent plastic strain gradient enhancement of single crystal plasticity: theory and numerics. *Proc. R. Soc. A* **2012**, *468*, 2682–2703.

18. Ling, C.; Forest, S.; Besson, J.; Tanguy, B.; Latourte, F. A reduced micromorphic single crystal plasticity model at nite deformations. Application to strain localization and void growth in ductile metals. *International Journal of Solids and Structures* **2018**, *134*, 143–169.
19. Scherer, J.M.; Besson, J.; Forest, S.; Hure, J.; Tanguy, B. Strain gradient crystal plasticity with evolving length scale: Application to voided irradiated materials. *European Journal of Mechanics A* **2019**, *77*, 103768.
20. Scherer, J.M.; Phalke, V.; Besson, J.; Forest, S.; Hure, J.; Tanguy, B. Lagrange multiplier based vs micromorphic gradient-enhanced rate-(in) dependent crystal plasticity modelling and simulation. *Computer Methods in Applied Mechanics and Engineering* **2020**, *372*, 113426.
21. Forest, S. Micromorphic approach for gradient elasticity, viscoplasticity, and damage. *Journal of Engineering Mechanics* **2009**, *135*, 117–131.
22. Sandström, R.; Hallgren, J.; Burman, G. Stress strain flow curves for Cu-OFP. *SKB Rapport R-09-14* **2009**.
23. Cordero, N.; Forest, S.; Busso, E. Micromorphic modelling of grain size effects in metal polycrystals. *Gesellschaft für Angewandte Mathematik und Mechanik* **2013**, *36*, 186–202.
24. Scherer, J.M.; Hure, J. A size-dependent ductile fracture model: Constitutive equations, numerical implementation and validation. *European Journal of Mechanics A* **2019**, *76*, 135–145.